

Homopairing Possibilities of the DNA Base Adenine

R. E. A. Kelly,^{*,†} Y. J. Lee,[‡] and L. N. Kantorovich[†]

Department of Physics, School of Physical Sciences and Engineering, King's College London, Strand, London WC2R 2LS, United Kingdom, and New Materials and Components Research Center, Research Institute of Industrial Science and Technology, P.O. Box 135, Pohang 790-330, South Korea.

Received: February 24, 2005; In Final Form: April 22, 2005

Using calculations based on the ab initio density functional theory, we for the first time report all possible planar DNA base adenine homodimers. Two density functionals and both localized and plane wave basis sets were used, and the results are compared with previous quantum chemical and semiempirical calculations available for a few pairs. We find that there are 21 possible planar adenine pairs with variable binding energies ranging from -0.03 to -0.86 eV. More stable pairs are associated with two strong hydrogen bonds formed between the monomers, while the least stable pairs are characterized by two or one relatively weak bonds. We find that stable hydrogen bonds can be characterized by the difference charge density that shows well-developed regions of alternating excess and depletion of the electron charge similar to a “kebab” structure. The presented detailed information on all planar adenine pairs can be utilized, for example, in considering possible adenine monolayers seen on various surfaces.

1. Introduction

Adenine (one of the four DNA bases) has been seen to form monolayers on organic and transition metal surfaces because of the molecule's ability to form hydrogen bonds even when adsorbed to these surfaces at room temperature. This is not a unique observation, as many small molecules seem to have the ability to self-assemble (ref 1). Therefore, research into self-assembling superstructures¹ or two-dimensional (2D) “supramolecular architectures” formed on solid surfaces has been of great interest recently due to the potential uses in the realms of nanotechnology. In addition, the self-assembly of small organic bases at the solid–liquid interface may explain possible mechanisms of prebiotic evolution before sophisticated organic molecules were formed.^{2,3} The formation of symmetric superstructures of achiral molecules on molybdenite (or, more generally, mineral surfaces) was also suggested to be a key in the origin of optical asymmetry in biology.^{2,3}

The adenine superstructures formed depend on the temperature and the surface that they are adsorbed on. Adenine has been deposited onto various inorganic surfaces such as the molybdenite,² graphite,^{4,2} copper (110),⁵ copper (111),^{6–10} and gold (111)^{11,12} surfaces. Scanning probe methods such as scanning tunneling microscopy (STM) may seem to be ideal to study in detail the adenine superstructures. The adenine molecules are considered as lying flat on the copper⁸ and graphite¹³ surfaces at a considerable distance, indicating that any interaction between the surface and molecules should be less important than the interaction between the molecules. On all these surfaces, it was seen that a 2D hexagonal adenine network (monolayer) was formed. However, the atomic resolution for small organic molecules and their assemblies is presently not possible, so that theoretical calculations are the only way to determine their actual structures.

In a previous study of adenine deposited onto the copper (111) surface,⁹ many superstructures were found based on temperature and deposition rate. One-dimensional adenine chains, 2D hexagonal adenine networks similar to those observed on molybdenite and graphite, and double-chain structures were all seen.⁹ The formation of various superstructures suggests that many different intermolecular hydrogen-bonding patterns can occur, so all possibilities for adenine dimers should be considered. However, existing theoretical calculations were performed only on a limited number of pairs,^{5,10,13–16} and no systematic analysis has been done so far to identify and study all possibilities.

Therefore, in this work we provide a complete analysis of all possible planar-orientated adenine homopairs (section 3.1) using an ab initio density functional theory (DFT) method considered in some detail in section 2. To our knowledge, no previous ab initio work exists in which all the possible planar pairings of adenine were investigated.

2. Method

Most of the present calculations were performed by the ab initio SIESTA method,^{17,18} which utilizes localized atomic numerical basis sets and periodic boundary conditions. The effect of the core electrons was simulated by means of first-principles scalar-relativistic norm-conserving^{19,20} Troullier–Martins²¹ pseudopotentials factorized in the Kleinman–Bylander form.²² The nonlinear core–valence exchange–correlation scheme²³ is applied for all elements except for hydrogen. The corresponding cutoff radii, R_c , were determined variationally for each species to ensure the best agreement in the eigenvalues with the all-electron calculations. In all calculations, the DZP (double- ζ plus polarization orbitals) basis set was used with an energy cutoff of 10 meV (ref 24). We find that the large size of the basis set is essential to obtain realistic bonding between molecules.

We used both the Perdew, Becke, and Ernzerhof (PBE)²⁵ and Becke,²⁶ Lee, Yang, and Parr²⁷ (BLYP) generalized gradient

* Author to whom correspondence should be addressed. E-mail: ross.kelly@kcl.ac.uk.

[†] King's College London.

[‡] Research Institute of Industrial Science and Technology.

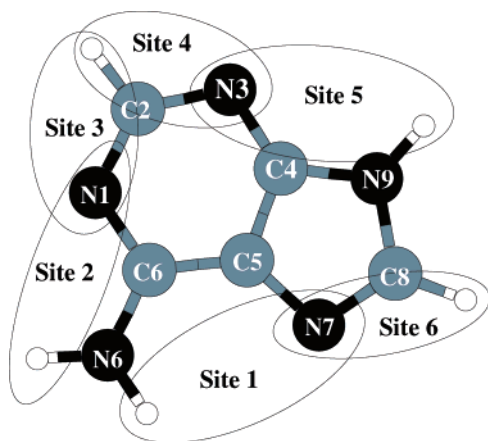


Figure 1. Adenine molecule in configuration A (top view). The configuration \bar{A} is obtained from A by flipping in the molecular plane. Atoms in the molecule are numbered as shown. The six possible pairs of nearest N and H atoms (bonding sites) that can participate in forming two adjacent hydrogen bonds between two adenine molecules are explicitly indicated.

approximations (GGA) for the exchange and correlation energy. It is generally assumed²⁸ that the BLYP functionals give a better description of the interactions in the hydrogen-bonded systems, while the PBE functional overestimates the hydrogen bonding between molecules in terms of geometry and stabilization energy. Therefore, our work should shed some light into usage of these density functionals for describing hydrogen-bonded systems.

Note that the reliability of DFT methods for small organic hydrogen-bonded dimers was questioned in some studies,^{15,29,30} but other work suggests that the use of DFT is more than appropriate for DNA bases and larger complexes.^{28,31–34} Good inclusion of electron correlation provided by the DFT methods enables one to avoid using the more computationally expensive post-Hartree–Fock methods.

The atomic relaxations in our calculations were performed until the forces on the atoms were not larger than 0.05 eV/Å and in some cases 0.01 eV/Å. In calculations on single molecules and dimers, very large supercells were used to avoid unphysical interaction between images. Therefore only one (gamma) \mathbf{k} -point has been found sufficient for our calculations.

Not much gas-phase experimental information is available on the DNA base geometry, so that we compared our results with previous ab initio studies performed using MP2³⁵ and DFT methods.³⁶ In general, we found a very good agreement in the adenine geometry with other ab initio work. We find that the adenine molecule is almost perfectly planar; see Figure 1. Spomer and Hobza³⁵ suggested amino group pyramidalisation due to sp^3 hybridization resulting in the two hydrogen atoms moving out of the molecular plane and the nitrogen atom moving in the opposite direction. They also suggested that the energy barrier for this out-of-plane displacement is very small. This has been confirmed in our calculations in which we constrained the amino group at various angles and found very small differences in energy that are comparable with the precision of our DFT calculations. Therefore, in all our work on dimers and monolayers, as initial geometries prior to relaxation, we have used the planar geometries obtained in the relaxation of a single molecule.

Another important characteristic is the dipole moment that exists in all four of the DNA bases. Adenine has the smallest dipole moment.¹⁵ Our SIESTA calculations gave 2.3 D, which is in reasonable agreement with the previous plane wave calculations³⁶ (2.56 D) and experiment³⁷ (2.5 D).

Thus, good agreement with previous ab initio calculations on the adenine molecule^{36,35} suggests that the pseudopotentials and basis set that we used are adequate for our purposes.

To analyze the stability of adenine pairs, we calculate a number of useful energies.³⁰ First, we use the *stabilization energy*, E_{stab} , defined as the total energy of the relaxed combined system (a pair) minus the total energies of all its individual components (two adenine molecules) relaxed separately. The combined system is stable if the $E_{\text{stab}} < 0$. To characterize the interaction between the two molecules, we define the *interaction energy*, E_{int} , as the total energy of the pair minus the energies of each individual molecule calculated in the geometry of the pair (without relaxation). This energy should also be negative for a stable system. Finally, we define the so-called *deformation energy*, $E_{\text{def}} = E_{\text{stab}} - E_{\text{int}}$, that characterizes the sum of losses in the total energies of the two molecules due to their relaxation in the pair. Since the individual energies of the molecules calculated in the geometry of the pair are higher than when they are allowed to relax individually, $E_{\text{def}} > 0$.

When calculating the stabilization energies using the SIESTA method, care should be taken since the localized basis set is used. In this case, it is essential that the basis set superposition error (BSSE³⁸) is to be accounted for to obtain reliable energetics in the calculations of pairs. These corrections have been calculated by the standard Boys–Bernardi counter-poise correction method.³⁸ To verify that this method is appropriate for our calculations of pairs, we have also performed some plane wave calculations on a number of pairs using the VASP code.^{39,40} In the latter case, similar large unit cells and the \mathbf{k} -point sampling were used as in the SIESTA calculations; however, we used ultrasoft pseudopotentials⁴¹ and the PBE density functional in all our VASP calculations. Recently, a number of small organic molecules have been successfully studied using the VASP code.³⁴

3. Results

3.1. Adenine Dimers: Energetics. It is generally accepted that for a stable dimer two or more hydrogen bonds must exist.^{42,43} In total, each molecule has eight atoms that have the ability to form a stable hydrogen bond: five hydrogen atoms (donors) and the three exposed N atoms (N1, N3, and N7 in Figure 1) as H acceptors. Due to the nearly round shape of the adenine molecule, only the two nearest donors or acceptors may participate in forming not more than two hydrogen bonds with another monomer. There is only a possibility of one hydrogen atom from each monomer forming a direct bond with another adenine because there are no hydrogen acceptors adjoining one another in the structure of adenine. Therefore, two hydrogen bonds may only be formed by adjacent H and N atoms, and there are six such pairs of atoms in each monomer as is clear from Figure 1. We shall refer to the adjacent pairs of N and H atoms as *bonding sites* in the following. Connecting every site of one molecule with every site of another, one obtains $(7 \times 6)/2 = 21$ possible dimers. Note that H atoms and H acceptors in every bonding site alternate.

Since the order of the adjacent N and H atoms in the molecule is not the same for all sites, not all pairs will be chiral. In fact, we find that there are 12 chiral and 9 nonchiral dimers. In the latter cases, one of the molecules should be flipped to facilitate the double hydrogen bond between two corresponding sites.

For instance, sites 1 and 5 can be bound together without flipping the second molecule (a chiral pair), while to bind the sites 1 and 6 it is necessary to flip the second molecule (a nonchiral pair). For convenience, the orientation of the molecule

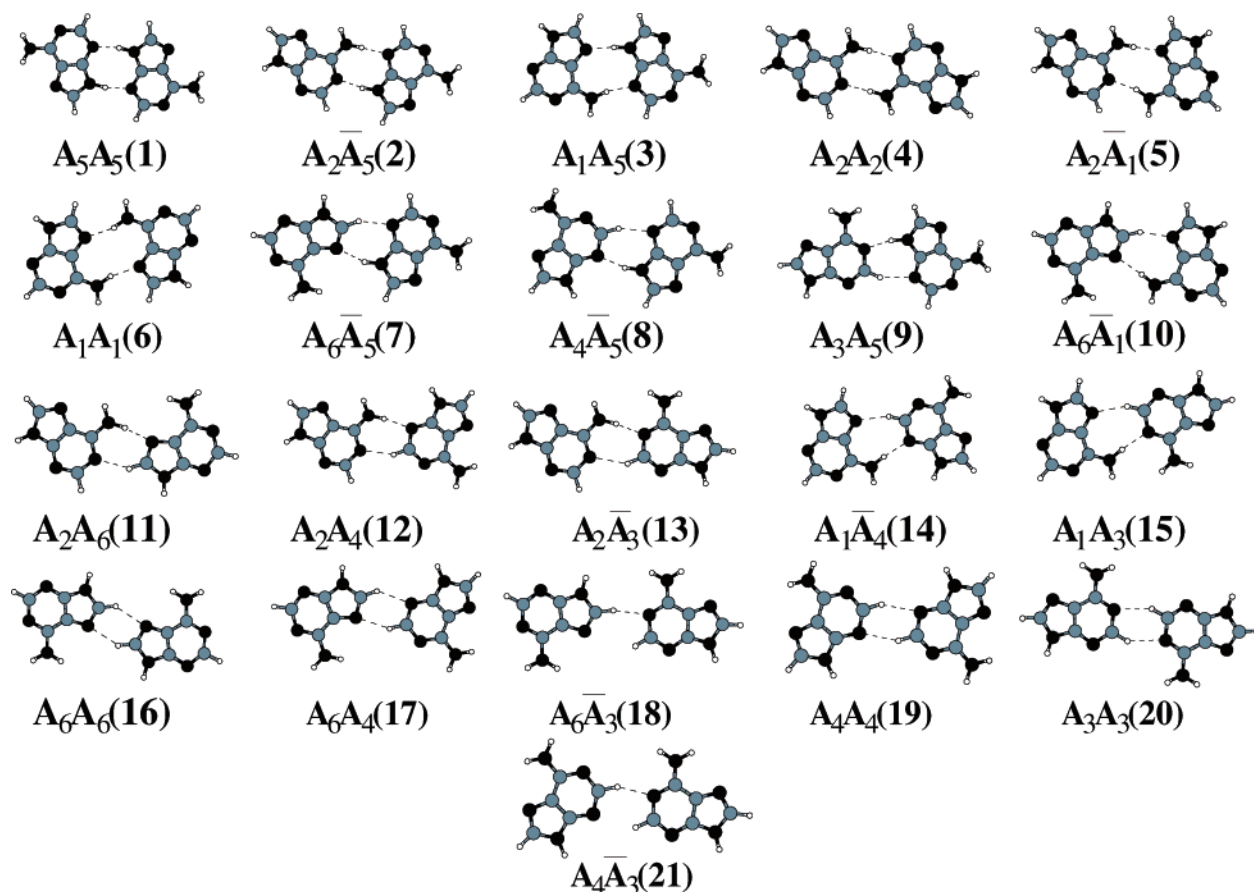


Figure 2. Relaxed adenine dimer structures in order of stability shown by the number in the round brackets. The notation A_nA_m corresponds to a dimer with chiral monomers, while $A_n\bar{A}_m$ corresponds to a pair with nonchiral monomers. The indices n and m indicate explicitly the sites of the two molecules (as adopted in Figure 1) engaged in the two hydrogen bonds in each pair.

shown in Figure 1 will be denoted A, while its nonchiral counterpart – \bar{A} . The relevant sites involved in the bonding of every pair will also be indicated explicitly, e.g., A_1A_5 or $A_1\bar{A}_6$ for the two examples of pairs above. Alternatively, we shall be using a single number (between 1 and 21), preceded by either AA or $\bar{A}\bar{A}$ symbols to indicate a particular dimer (either chiral or nonchiral, respectively), with all the dimers being ordered in terms of their binding energies calculated using the PBE functional, e.g., AA1 and AA9.

The relaxed geometries of all pairs are shown in Figure 2. These include six chiral centro-symmetric pairs (AA1, AA4, AA6, AA16, AA19, and AA20) built using the same sites on each monomer, i.e., A_nA_n ; they each have C_2 symmetry. Previous dimer calculations were based on different philosophies. The six centro-symmetric adenine dimers were identified by Chen et al.⁵ from the observed C_2 symmetry of the monolayer domains. Furukawa et al.,¹⁰ using an entropy argument, considered only the most stable five pairings (AA1–AA5). All 21 adenine dimers have been calculated in this work for the first time.

Note that all adenine pairs exhibit very near-planar geometries. The stabilization, interaction, deformation, and BSSE energies of all the adenine dimers are given in Table 1 for the PBE and BLYP GGA functionals calculated using the SIESTA method. The pair A_5A_5 (or AA1) is the most stable. We note that the stabilization energies calculated with both functionals are very close, and almost the same energetic ordering of pairs is observed. In both cases, the BSSE corrections were found to be significant, especially for the less energetically favorable pairs. Note that the stabilization energies of the least stable pairs (the bottom three entries in the table) are on the order of the

precision of our method. In these cases, the interaction between the two molecules is extremely weak.

The deformation energies of different pairs are quite small, indicating that atomic relaxation within each molecule is not significant and can be neglected to a good approximation. This is in agreement with previous pair calculations.⁴⁴ The absolute values of the deformation and interaction energies generally increase as the stabilization energy increases, which was also observed in the MP2 study of DNA base pairs.¹⁵

If we compare different sites (Figure 1 and Table 1) in their abilities to form stable dimers, site 5 (involved in the top three pairs) and then sites 2 and 1 seem to be the most efficient for bonding. At the same time, sites 3 and 4, followed by site 6, are involved in most of the less energetically favorable pairs (the bottom of the list in Table 1).

The stabilization energies found in this study, shown in Table 1, are quite similar to those calculated using the MP2 method¹⁶ and the semiclassical Dreiding II force field method.¹³ The recent benchmark calculations¹⁶ for nucleic acid pairs were performed using MP2 geometry optimization with higher-level correlation effects included posteriori for the energy. Their absolute stabilization energies are seen to be consistently lower than ours but not by a significant amount (0.06 eV), and the ordering is the same. The semiclassical approach of ref 13 gave also a good agreement in the stabilization energies for the three pairs AA4, AA5, and AA6. However, a worse agreement is observed for the first pair AA1 that has its stabilization energy underestimated by -0.25 eV, which results in the wrong ordering of the pairs. The energetic ordering of pairs in the calculations based on the semiempirical PM3 method¹⁰ is the same as in our calculations; however, the stabilization energies

TABLE 1: Adenine Base Pair Energies (in eV) Calculated Using PBE and BLYP Density Functionals^a

pair	PBE				BLYP				E_{stab} (literature)			
	E_{BSSE}	E_{int}	E_{def}	E_{stab}	E_{BSSE}	E_{int}	E_{def}	E_{stab}	ref 16	ref 13	ref 10	ref 5
A ₅ A ₅ (1)	0.16	-1.03	0.17	-0.86	0.15	-0.85	0.05	-0.79		-0.62	-0.34	-0.44
A ₂ A ₅ (2)	0.15	-0.87	0.17	-0.70	0.14	-0.87	0.15	-0.72			-0.18	
A ₁ A ₅ (3)	0.15	-0.80	0.15	-0.66	0.14	-0.82	0.12	-0.69			-0.17	
A ₂ A ₂ (4)	0.14	-0.73	0.15	-0.58	0.13	-0.73	0.14	-0.60	-0.51	-0.64	-0.14	-0.19
A ₂ A ₁ (5)	0.14	-0.66	0.12	-0.54	0.13	-0.69	0.12	-0.57	-0.48	-0.55	-0.13	
A ₁ A ₁ (6)	0.14	-0.55	0.08	-0.47	0.12	-0.60	0.11	-0.49	-0.41	-0.51		-0.27
A ₆ A ₅ (7)	0.12	-0.49	0.05	-0.43	0.09	-0.57	0.10	-0.47				
A ₄ A ₅ (8)	0.12	-0.41	0.05	-0.36	0.12	-0.47	0.07	-0.40				
A ₃ A ₅ (9)	0.12	-0.43	0.07	-0.36	0.11	-0.49	0.08	-0.40				
A ₆ A ₁ (10)	0.11	-0.39	0.06	-0.33	0.11	-0.45	0.09	-0.35				
A ₂ A ₆ (11)	0.11	-0.38	0.06	-0.32	0.10	-0.45	0.11	-0.35				
A ₂ A ₄ (12)	0.10	-0.30	0.04	-0.27	0.10	-0.38	0.08	-0.31				
A ₂ A ₃ (13)	0.10	-0.30	0.04	-0.26	0.10	-0.38	0.09	-0.29				
A ₁ A ₄ (14)	0.11	-0.31	0.05	-0.25	0.11	-0.38	0.08	-0.30				
A ₁ A ₃ (15)	0.11	-0.29	0.05	-0.24	0.10	-0.37	0.09	-0.28				
A ₆ A ₆ (16)	0.07	-0.18	0.01	-0.17	0.06	-0.28	0.10	-0.18				-0.03
A ₆ A ₄ (17)	0.07	-0.11	0.01	-0.10	0.07	-0.06	0.01	-0.04				
A ₆ A ₃ (18)	0.05	-0.10	0.01	-0.09	0.05	-0.24	0.12	-0.12				
A ₄ A ₄ (19)	0.06	-0.07	0.01	-0.06	0.06	-0.12	0.02	-0.10				-0.03
A ₃ A ₃ (20)	0.06	-0.07	0.01	-0.06	0.07	-0.10	0.01	-0.09				0.02
A ₄ A ₃ (21)	0.07	-0.04	0.01	-0.03	0.06	-0.02	0.02	0.00				

^a E_{int} , E_{def} , and E_{stab} are the interaction, deformation, and stabilization energies, respectively, while E_{BSSE} corresponds to the BSSE correction. Results of our calculations are compared with other available work presented in the last four columns.

TABLE 2: Adenine Pair Energies (in eV) Calculated Using the VASP and SIESTA Methods for a Selection of Five Pairs from Figure 2^a

pair	VASP			SIESTA		
	E_{int}	E_{def}	E_{stab}	E_{int}	E_{def}	E_{stab}
A ₅ A ₅ (1)	-0.96	0.15	-0.81	-1.02	0.17	-0.86
A ₁ A ₁ (6)	-0.54	0.11	-0.42	-0.54	0.08	-0.46
A ₆ A ₁ (10)	-0.39	0.09	-0.30	-0.39	0.06	-0.33
A ₆ A ₃ (18)	-0.11	0.05	-0.06	-0.10	0.01	-0.09
A ₄ A ₃ (21)	-0.07	0.05	-0.02	-0.04	0.01	-0.03

^a In either case the PBE exchange–correlation functional was used. E_{int} , E_{def} , and E_{stab} are the interaction, deformation, and stabilization energies, respectively.

are largely underestimated. Similarly, very poor agreement with our ab initio calculations is observed in energies obtained using another semiempirical method reported in ref 5. These comparisons suggest that one has to use semiempirical approaches with care, which was previously reported in ref 45.

To verify if the basis set that we used in the SIESTA calculations is sufficiently large, a sample of five dimers with varying stabilization energies has been also calculated using the VASP code as explained in section 2. Since plane waves are used in the VASP calculations, the convergence with respect to the basis set can easily be achieved by simply increasing the cutoff energy. No BSSE correction is required with plane waves because the basis set is complete. However, the calculations are much more demanding due to the large cell sizes used. The stabilization, interaction, and deformation energies for the chosen dimers calculated using the VASP and SIESTA employing similar size supercells, **k**-point sampling, and the PBE density functional are compared in Table 2. The obtained agreement is extremely good, indicating that the finite local basis set that we used in our SIESTA calculations is appropriate. Note that the agreement would have been much worse had we not used the BSSE correction in our SIESTA calculations.

3.2. Adenine Pairs: Geometry. The strength of the hydrogen bonds in the dimers can be correlated with the geometry at which two molecules bind to each other. In each dimer, two hydrogen bonds are created. Each bond can be characterized by the donor–acceptor (N–H–N or N–H–C) distance and the angle

(either N–H–N or N–H–C, depending on the atom immediately connected to the donor H atom in one of the molecules). It should be stressed that the hydrogen-bonding strength cannot be entirely analyzed just by using its geometrical characteristics since all atoms must be taken into account when analyzing dimers.^{14,15} Still, the geometry of each pair provides useful information about the dimer formation.

The distances for the two bonds and the corresponding angles are shown for each dimer in Table 3 in which the dimers are ordered in the same way as in Table 1. It is seen that stronger bonds are on average correlated with shorter distances and with angles approaching 180° although these correlations are not uniform across the whole list of dimers. This cooperativity or combined supportive nature of the hydrogen bonds was also stressed in the previous calculations of ref 44. Two linear hydrogen bonds would be the preferred option for a pair, but this is not available due to the particular shapes of the two molecules, which also reinforces the idea of rigidity of the DNA bases in pair structures.⁴⁴

Another interesting point to include here is that in two relaxed pair structures (A₅A₁₈ and A₄A₂₁) the two C–N–H distances (Table 3) are quite different, with one in each case being much longer than the other. It may be said that in these two cases only one hydrogen bond is formed, contrary to the common belief that two or more hydrogen bonds can only form a stable pair. Note, however, that in these two cases the stabilization energy is very small.

When comparing with the results of the Hartree–Fock (HF) geometry optimization calculations of adenine dimers by Sponer et al.¹⁵ (see the last two columns in Table 3), we see that the angles are very similar in the two calculations. However, our H–N distances are found to be consistently smaller (by ≈0.1 Å), which is likely to be due to the fact that in our calculations the correlation effects have been also accounted for during the geometry optimization. It is seen from the table that the bond lengths systematically decrease from the HF geometry optimization results¹⁵ if the MP2 geometry optimization was employed.¹⁶ This tendency qualitatively agrees with our DFT calculations.

It is usually expected that the BLYP set of functionals is the most appropriate one for describing the hydrogen bond and

TABLE 3: Geometrical Characteristics (in Å and deg) of Two Hydrogen Bonds in Each Adenine Pair Calculated Using the PBE and BLYP Density Functionals

pair	hydrogen bond	PBE (SIESTA)		BLYP (SIESTA)		PBE (VASP)		ref 16	ref 15	
		length	angle	length	angle	length	angle	length	length	angle
A ₅ A ₅ (1)	N9—H···N3	2.76	169.1	2.83	169.0	2.83	169.7			
	N9—H···N3	2.76	169.1	2.83	169.0	2.83	169.7			
A ₂ A ₅ (2)	N6—H···N3	2.81	175.7	2.82	176.0					
	N9—H···N1	2.79	168.8	2.81	168.9					
A ₁ A ₅ (3)	N6—H···N3	2.85	169.0	2.86	169.4					
	N9—H···N7	2.80	174.3	2.81	174.3					
A ₂ A ₂ (4)	N6—H···N1	2.83	178.0	2.81	178.2			2.95	3.16	179.4
	N6—H···N1	2.83	178.0	2.81	178.2			2.95	3.16	179.4
A ₂ A ₁ (5)	N6—H···N7	2.82	177.3	2.83	176.8			2.96	3.16	175.1
	N6—H···N1	2.86	167.9	2.88	168.1			2.95	3.17	163.3
A ₁ A ₁ (6)	N6—H···N7	2.90	163.8	2.91	164.8	2.96	161.6	2.96	3.18	158.4
	N6—H···N7	2.90	163.8	2.91	164.8	2.96	161.6	2.96	3.18	158.4
A ₆ A ₅ (7)	C8—H···N3	3.09	153.4	3.18	153.0					
	N9—H···N7	2.87	159.6	2.92	160.3					
A ₄ A ₅ (8)	C2—H···N3	3.23	158.1	3.26	159.9					
	N9—H···N3	2.88	163.3	2.88	162.9					
A ₃ A ₅ (9)	C2—H···N3	3.24	155.4	3.30	155.3					
	N9—H···N1	2.80	163.9	2.84	164.5					
A ₆ A ₁ (10)	N6—H···N7	2.98	176.0	2.95	175.0	3.02	173.2			
	C8—H···N7	3.15	156.6	3.15	157.3	3.24	153.7			
A ₂ A ₆ (11)	C8—H···N1	3.09	146.8	3.23	146.4					
	N6—H···N7	2.86	168.1	2.88	169.0					
A ₂ A ₄ (12)	N6—H···N3	2.89	172.8	2.90	173.0					
	C2—H···N1	3.27	148.4	3.39	148.3					
A ₂ A ₃ (13)	N6—H···N1	2.88	174.6	2.89	174.7					
	C2—H···N1	3.34	146.9	3.47	147.0					
A ₁ A ₄ (14)	N6—H···N3	2.98	175.9	2.94	173.6					
	C2—H···N7	3.23	158.7	3.26	159.0					
A ₁ A ₃ (15)	N6—H···N1	2.95	173.9	2.96	173.9					
	C2—H···N7	3.21	156.0	3.28	155.9					
A ₆ A ₆ (16)	C8—H···N7	3.30	142.4	3.44	145.6					
	C8—H···N7	3.30	142.4	3.44	145.6					
A ₆ A ₄ (17)	C2—H···N7	3.29	147.6	3.39	147.6					
	C8—H···N3	3.27	137.7	3.46	137.5					
A ₆ A ₃ (18)	C8—H···N1	3.21	167.1	3.24	166.8	3.36	167.1			
	C2—H···N7	3.99	133.5	4.26	133.7	4.12	134.8			
A ₄ A ₄ (19)	C2—H···N3	3.44	147.7	3.30	147.5					
	C2—H···N3	3.44	147.7	3.30	147.5					
A ₃ A ₃ (20)	C2—H···N1	3.33	149.0	3.35	148.8					
	C2—H···N1	3.33	149.0	3.35	148.8					
A ₄ A ₃ (21)	C2—H···N1	3.20	153.7	3.43	153.8	3.65	139.1			
	C2—H···N3	3.47	139.0	3.78	140.6	3.39	152.6			

^a Each bond is presented via the distance between the H donor atom of one molecule and the corresponding acceptor N atom of another. Also, the angle between the X—H atoms of the first molecule and the N atom of another is shown, where X, depending on the particular dimer, is either C or N. Numbering of atoms is identical to that adopted in Figure 1. In the last three columns, results of our calculations are compared with those found in refs 15 and 16 using the HF and MP2 geometry optimization methods, respectively.

hydrogen-bonded systems.²⁸ We find in our calculations that the PBE functional performs equally well; the stabilization energies are very similar, almost exactly the same ordering of dimers has been obtained, and the H—N distances and hydrogen bond angles also agree well. Note that consistently longer bond distances in the BLYP calculations were found as compared to the PBE ones.

3.3. Adenine Pairs: Electron Density. To visualize the hydrogen bonding in the dimers, one may look at the electron density. We found, however, that the total electron density is not very informative. A much more convenient quantity that can be used to characterize the hydrogen bonding is the one that we shall call the *interaction density*. It is defined as the difference $\Delta\rho = \rho_{AB} - (\rho_A + \rho_B)$, where ρ_{AB} is the electron density of the combined system (a pair), while ρ_A and ρ_B are the densities of its individual parts (monomers) calculated using the geometry of the combined system AB. The latter point is essential to avoid apparent density changes due to atomic relaxation. It may appear that the same quantity (called the regular deformation density) was also used in ref 46, although

the authors did not state clearly if the densities ρ_A and ρ_B were calculated at the geometry of the pair AB.

The interaction densities of three dimers, including the most stable pair AA1, the least stable pair AA21, and the pair AA10 of intermediate stability, are shown in Figure 3. Let us first discuss the most stable pair AA1 shown in Figure 3a. We see that the bonding does indeed involve many atoms including those that are not directly involved in the hydrogen bonds. There is a charge redistribution across the two molecules, although it is very small (on the order of ± 0.01 of the electron charge). Still one can clearly see alternating regions of excess and depletion of the charge density of the dimer across the two hydrogen bonds, i.e., each bond has a characteristic “kebab” structure. These findings reinforce a general perception of this interaction to be of a weak electrostatic nature. The study by Guerra et al., which studied the hydrogen bonding between DNA base pairs, has previously shown this sort of interaction between complementary DNA base pairs (Figure 11 in ref 47).

The interaction density for the next pair AA10 shown in Figure 3b has a well-defined (and strong) N—H—N bond,

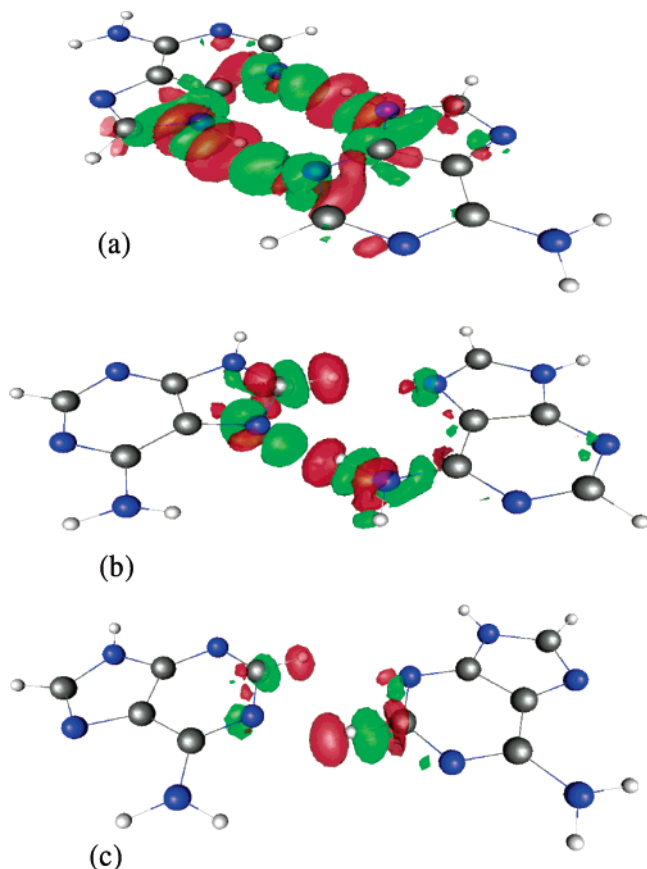


Figure 3. Interaction density of the (a) AA1, (b) AA10, and (c) AA21 pairs calculated using the PBE functional as implemented in the SIESTA method for the electron density difference of ± 0.01 electrons. The green surface corresponds to regions of positive electron density difference (i.e., charge excess areas) and the red areas correspond to regions of negative electron density difference (charge depletion areas).

whereas the C–H–N bond is much less pronounced and must be much weaker. This agrees with the fact that the C–H–N bond length is much longer in this case than the one for the other N–H–N bond; see Table 3. Finally, the weakest pair AA21 shown in Figure 3c has an incomplete “kebab” structure for both bonds. Still a few regions of alternating charge density are clearly visible there, and these must be responsible for a very small stabilization energy for this pair found in our calculations. This result suggests that, despite the insufficient precision of the present calculations, we still can conclude that this pair is weakly stable. Therefore, the lower-energy pairs may also be included when considering larger adenine structures.

Note that essentially identical results for the electron density were obtained using the BLYP functional with the SIESTA code and the PBE functional using the VASP code. Therefore, as the “kebab” structure of the hydrogen bond is found independent of the basis set used and the particular density functional, it can be considered as a characteristic *signature* of the hydrogen bonding.

4. Discussion and Conclusions

In this work, we have considered, using an *ab initio* DFT method, all possible adenine pairs stabilized by two hydrogen bonds. We find that 21 pairs are possible with the stabilization energies spanning a wide interval from just below 0 to -0.86 eV. Five pairs have stabilization energies on the order of -0.1 eV or less, nine between -0.15 and -0.36 eV, and the remaining seven pairs (from AA1 to AA7) have the highest

stabilization energies ranging between -0.43 and -0.86 eV, the centro-symmetric pair AA1 being the most energetically favorable. We find a certain correlation between the stabilization energies and the geometry of the hydrogen bonds formed; generally, the pair is more stable if the distances between the donor and acceptor atoms are smaller and the bond is more linear. Two density functionals (PBE and BLYP) and both localized and plane wave basis sets have been used, giving very similar results.

Only a limited amount of previous theoretical work on the adenine pairs can be found in the literature. In particular, only a small subset of the pairs considered in this work is available, and our calculations agree very well with the benchmark calculations performed on these using *ab initio* quantum chemistry methods.¹⁶ We suggest that the accuracy of the DFT methods is more than appropriate for these DNA bases.

We also find, in agreement with the previous results of ref 45, that there is a rather bad agreement of our calculations with available previous semiempirical work. Even though the energetic ordering of the pairs is similar, it is not the same, and different semiempirical methods give varying results. In addition to these disagreements, the semiempirical methods largely underestimate the stabilization energies of all pairs. Similarly, a semiclassical method (see, e.g., ref 13) predicts that the AA4 pair is more stable than the AA1 dimer, which is at variance with our results. Therefore, one has to be extremely careful in using those methods in studying the geometry and energetics of the DNA base molecules and larger structures formed by these small organic molecules.

Deformation energies calculated for the pairs have been found to be not very significant, indicating that molecules can be considered as rigid in the pairs to the first approximation. This conclusion agrees with the previous work.⁴⁴ Note, however, that the deformation of molecules adsorbed on a surface may change the bonding strength in the pairs, so that for surface-based monolayer calculations the surface–substrate interaction needs to be understood initially.

We have also analyzed the electron density for all the pairs. We find that pairs with strong bonding (e.g., the AA1 pair) demonstrate a specific electron charge redistribution in the form of alternating rings of excess and depletion of the electron density along the hydrogen bond resembling a “kebab” structure. This can be considered as a characteristic signature of the hydrogen bond, and similar results have been obtained in other high-quality DFT calculations of the DNA complementary pairs adenine–thymine and cytosine–guanine.⁴⁷ In the case of weakly bound adenine pairs, however, we find that the “kebab” structure is formed only partially or may not be visible at all for one of the two bonds.

The information gained from our dimer calculations should help in building up all possible gas-phase monolayers of adenine monomers. It follows from our calculations that different adenine sites have different abilities to form a hydrogen bond. Six centro-symmetric pairs have been obtained, the most stable one being the AA1 pair, although only three of these can be considered as having significant stabilization energies. Centro-symmetric pairs are thought to be important for monolayer construction because the dipole moments would effectively cancel one another.³ It is widely believed that the AA1 pair is the most likely basis of any monolayer that is observed on the Cu(111)^{8–10} and Cu(110)⁵ surfaces. Note, however, that as far as monolayers are concerned, these cannot be formed entirely by employing only the most energetically favorable pairs since each monomer is connected to three of its neighbors in a hexagonal network.

There should be a subtle balance between the favorable and less favorable hydrogen bonds in the monolayer to saturate all necessary links between molecules, and thus all types of dimers should be considered for possible pairings in monolayers.

Acknowledgment. We are extremely grateful to Mark Green, Roberto Otero, and Maya Stock for many useful discussions and Christopher Hobbs for his help in setting up the SIESTA calculations. We also acknowledge the computer time on the HPCx supercomputer provided via the Materials Chemistry Consortium. R.E.A.K. is also grateful to the EPSRC for financial support (Grant No. GR/P01427/01).

References and Notes

- (1) De Feyter, S.; De Schryver, C. *Chem. Soc. Rev.* **2003**, 32, 139.
- (2) Sowerby, S. J.; Heckl, W. M.; Petersen, G. B. *J. Mol. Evol.* **1996**, 43, 419.
- (3) Sowerby, S. J.; Heckl, W. M. *Origins Life Evol. Biosphere* **1998**, 28, 283.
- (4) Freund, J. E.; Edelwirth, M.; Krobek, P.; Heckl, W. M. *Phys. Rev. B* **1997**, 55, 5394.
- (5) Chen, Q.; Frankel, D. J.; Richardson, N. V. *Langmuir* **2002**, 18, 3219.
- (6) Tanaka, H.; Nakagawa, T.; Kawai, T. *Surf. Sci.* **1996**, 364, L575.
- (7) Kawai, T.; Tanaka, H.; Nakagawa, T. *Surf. Sci.* **1997**, 386, 124.
- (8) Furukawa, M.; Tanaka, H.; Kawai, T. *Surf. Sci.* **1997**, 392, L33.
- (9) Furukawa, M.; Tanaka, H.; Kawai, T. *Surf. Sci.* **2000**, 445, 1.
- (10) Furukawa, M.; Tanaka, H.; Kawai, T. *J. Chem. Phys.* **2001**, 115, 3419.
- (11) Otero, R.; Schock, M. Private communication.
- (12) Tao, N. J.; DeRose, J. A.; Lindsay, S. M. *J. Phys. Chem.* **1993**, 97, 910.
- (13) Edelwirth, M.; Freund, J.; Sowerby, S. J.; Heckl, W. M. *Surf. Sci.* **1998**, 417, 201.
- (14) Hobza, P.; Sandorfy, C. *J. Am. Chem. Soc.* **1987**, 109, 1302.
- (15) Sponer, J.; Leszczynski, J.; Hobza, P. *J. Phys. Chem.* **1996**, 100, 1965.
- (16) Sponer, J.; Jurecka, P.; Hobza, P. *J. Am. Chem. Soc.* **2004**, 126, 10142.
- (17) Ordejon, P.; Artacho, E.; Soler, J. M. *Phys. Rev. B* **1996**, 53, R10441.
- (18) Soler, J. M.; Artacho, E.; Gale, J. D.; Garcia, A.; Junquera, J.; Ordejon, P.; Sanchez-Portal, D. *J. Phys.: Condens. Matter* **2002**, 14, 2745.
- (19) Kleinman, L. *Phys. Rev. B* **1980**, 21, 2630.
- (20) Bachelet, G. B.; Schluter, M. *Phys. Rev. B* **1982**, 25, 2103.
- (21) Troullier, N.; Martins, J. L. *Phys. Rev. B* **1991**, 43, 1993.
- (22) Kleinman, L.; Bylander, D. M. *Phys. Rev. Lett.* **1982**, 48, 1425.
- (23) Louie, S. G.; Froyen, S.; Cohen, M. L. *Phys. Rev. B* **1982**, 26, 1738.
- (24) Artacho, E.; Sanchez-Portal, D.; Ordejon, D.; Garcia, A.; Soler, J. M. *Phys. Status Solidi B* **1999**, 215, 809.
- (25) Perdew, J. P.; Burke, K.; Ernzerhof, M. *Phys. Rev. Lett.* **1996**, 77, 3865.
- (26) Becke, A. D. *Phys. Rev. A* **1988**, 38, 3098.
- (27) Lee, C.; Yang, W.; Parr, R. G. *Phys. Rev. B* **1988**, 37, 785.
- (28) Segall, M. D. *J. Phys.: Condens. Matter* **2002**, 14, 2957.
- (29) Sponer, J.; Leszczynski, J.; Hobza, P. *THEOCHEM* **2001**, 573, 43.
- (30) Sponer, J.; Leszczynski, J.; Hobza, P. *Biopolymers* **2001**, 61, 3.
- (31) Artacho, E.; Machado, M.; Sanchez-Portal, D.; Ordejon, P.; Soler, J. M. *Mol. Phys.* **2003**, 101, 1587.
- (32) Felice, D. R.; Calzolari, A.; Molinari, E.; Garbesi, A. *Phys. Rev. B* **2001**, 65, 045104.
- (33) Gu, J.; Leszczynski, J. *Chem. Phys. Lett.* **2001**, 335, 465.
- (34) Sun, G.; Kurti, J.; Rajczy, P.; Kertesz, M.; Hafner, J.; Kresse, G. *THEOCHEM* **2003**, 624, 37.
- (35) Sponer, J.; Hobza, P. *J. Phys. Chem.* **1994**, 98, 3161.
- (36) Preuss, M.; Schmidt, W. G.; Seino, K.; Furthmuller, J.; Bechstedt, F. *J. Comput. Chem.* **2004**, 25, 112.
- (37) DeVoe, H.; Tinoco, I. J. *J. Mol. Biol.* **1962**, 4, 500.
- (38) Boys, S. F.; Bernardi, F. *Mol. Phys.* **1970**, 19, 553.
- (39) Kresse, G.; Hafner, J. *Phys. Rev. B* **1993**, 47, 558.
- (40) Kresse, G.; Furthmuller, J. *J. Comput. Mater. Sci.* **1996**, 6, 15.
- (41) Kresse, G.; Hafner, J. *J. Phys.: Condens. Matter* **1994**, 6, 8245.
- (42) Watson, J. D.; Crick, F. H. C. *Nature* **1953**, 171, 737.
- (43) Saenger, W. *Principles of Nucleic Acid Structure*; Springer: New York, 1984.
- (44) Asensio, A.; Kobko, N.; Dannenberg, J. J. *J. Phys. Chem. A* **2003**, 107, 6441.
- (45) Hobza, P.; Kabelac, M.; Sponer, J.; Mejzlik, P.; Vondrasek, J. *J. Comput. Chem.* **1997**, 18, 1136.
- (46) Bickelhaupt, F. M.; Van Eikema Hommes, N. J. R.; Guerra, C. F.; Baerends, E. J. *Organometallics* **1996**, 15, 2923.
- (47) Guerra, C. F.; Bickelhaupt, F. M.; Snijders, J. G.; Baerends, E. J. *Chem.—Eur. J.* **1999**, 5, 3581.